

https://dspace.org/

Designing Parameters of SurfactantFree Electrochemical Sensors for Dopamine and Uric Acid on Nitrogen Doped Graphene Films

Boitumelo Matsoso; Tsenolo Lerotholi; Neil Coville; Glenn Jones

https://hdl.handle.net/10539/35047
ISI

Downloaded from a DSpace repository. https://dspace.org/

https://doi.org/10.1595/205651319X15472048744138 *Johnson Matthey Technol. Rev.*, 2019, **63**, (2), 76–88

JOHNSON MATTHEY
TECHNOLOGY REVIEW

www.technology.matthey.com

Designing Parameters of Surfactant-Free Electrochemical Sensors for Dopamine and Uric Acid on Nitrogen Doped Graphene Films

Evaluating the correlation between the content of N-configurations and the sensing for electrochemically active molecules

Boitumelo J. Matsoso*§, Tsenolo Lerotholi, Neil J. Coville
DST-NRF Centre of Excellence in Strong Materials and The Molecular Sciences Institute, School of Chemistry, University of the Witwatersrand, Private Bag 3, PO WITS, 2050, South Africa

§Present address: Laboratoire des Multimatériaux et Interfaces-UMR 5615 CNRS/ UCBL, Domaine Scientifique de la Doua, Université Claude Bernard Lyon 1 Bâtiment Chevreul, 6 rue Victor Grignard, 69622 Villeurbanne cedex, France

Glenn Jones**
Johnson Matthey, Blounts Court, Sonning Common, Reading, RG4 9NH, UK

Email: *boitumelo.matsoso@univ-lyon1.fr and **gjones@matthey.com

Electrochemistry studies on the derivatives of graphene have been in the forefront of chemical research in recent years. The large specific surface area, high electrical conductivity, fast electron transfer rate and excellent biocompatibility to biomolecules constitute a few of the underlying reasons for the extensive application of graphene derivatives in modern electrochemistry and related technologies. Much interest in graphene derivatives has been driven by the ease of intentional functionalisation of the carbon backbone of graphene with dopants, such as nitrogen. Doping enhances the electrical conductivity and biocompatibility of nitrogen-doped graphene (NGr) nanomaterials and aids in their potential applications in electrochemical sensing and spectroelectrochemical devices. Despite the application of NGr in electrochemical sensing devices, the major challenge for reproducible industrial application still lies in the use of surfactants and binders and the limited knowledge on the correlation between the N-configurations and the electrocatalytic performance of these NGr-based electrodes. Therefore, the purpose of this short review article is to highlight some recent progress on the application of NGr derivatives for electrochemical detection of biomarkers such as uric acid and dopamine. The paper will also illustrate design parameters for new surfactant-free two-dimensional (2D) N-doped graphene based electrochemical sensors with variable N-functionalities for the detection of dopamine and uric acid.

1. Introduction

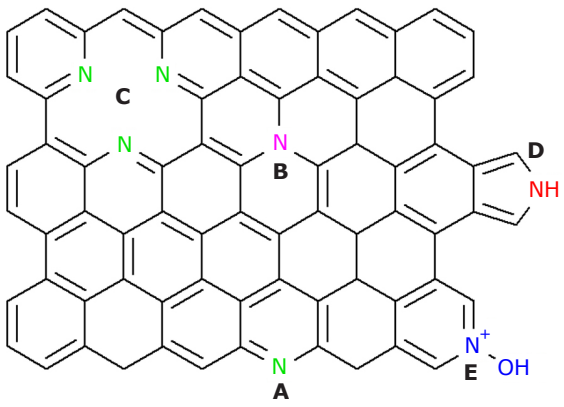
In recent years, the ever-growing demand for efficient and cost-effective disease diagnosis in order to improve the quality of life for today's global community is greatly sought after. One of the many ways to achieve the aforementioned demand has been through the use of electrochemical methods for environmental monitoring, disease diagnosis, detection of drugs in pharmaceutical assays or biological fluids and energy storage (1–8). The search for 'better' electrode materials suitable for employment in electrochemical methods in various

© 2019 Johnson Matthey

scientific disciplines, for the present day needs of science and society, is increasing (7–15). The term 'better' here relates to electrodes which are robust and have higher conductivity, excellent selectivity and enhanced sensitivity. The electrodes must also be non-poisonous, should involve simple preparation procedures and be cost-effective. A wide range of electroactive molecules and biological species that have been studied by electrochemical techniques include the detection of dopamine (DA) and uric acid (UA); solely due to their vital roles in metabolic and physiological processes in human bodies (5–7, 16–24). For instance, abnormal levels of DA and UA are a powerful indicator for the diagnosis of Parkinson's disease, schizophrenia, gout, Lesch-Nyhan syndrome and lymphoma (24–27). Thus, the rapid and accurate electrochemical detection of DA, UA and their metabolites, at nanomolar concentrations, is required not only for clinical diagnosis but also for the prevention of disorders arising from their deficiencies.

Despite the good sensitivity displayed by electrochemical methods for the detection of DA and UA, severe overlap of the oxidation potentials of DA and UA with other molecules like ascorbic acid (AA) (1–15) at conventional electrodes remains a problem. Additionally, the frequent replacement of traditional electrodes due to fouling (28–30) is a major contributing factor during the detection of UA. To address these problems, considerable research efforts have been devoted to the improvement of the electrode surfaces as well as the development of new electrode materials that can separate the signal potentials of DA, UA, AA and other molecules. This includes the use of various nanomaterials such as metals and metal oxides, carbon nanomaterials and magnetic nanoparticles (31–38). Among the commonly used carbon nanomaterials, derivatives of graphene have played tremendous roles in electronics, electrochemistry and sensor communities. Recent research on the electrochemistry of graphene-based nanomaterials has shown that these structures have excellent electrocatalytic activity, good biocompatibility with amino acids and proteins, extraordinary conductivity and a large specific surface area (39, 40). The ultimate interest for the employment of graphene-based nanomaterials in electrochemical sensors is based on the charge-active (bio)molecule interactions at π-π domains. Additionally, intentional tailoring of the electronic and electrochemical properties of graphene through the incorporation of p-block elements such as nitrogen, in the form of pyridinic-, pyrrolic-, graphitic-N and oxidised pyridinic-N (**Scheme I**) (41), has been found to be a promising method for improving the performance of graphene-based electrochemical sensors (42–46). For instance, theoretical and experimental studies have indicated that high concentrations of both pyridinic and pyrrolic N-configurations improve the biocompatibility of N-graphene materials through enhanced hydrogen bonding as well as through the π-π interactions between the graphene and the electroactive molecule (47, 48).

Thus introduction of N atoms into the carbon backbone of graphene could enable the electrocatalytic performance and biocompatibility of N-graphene based sensors to be easily tuned by controlling the amount of each N configuration. However, little information has been documented on the effect of relative concentrations of each N-configuration on the subsequent electrocatalytic performance of N-graphene based electrochemical sensors. Therefore, the aim of this article is to summarise the progress on recently developed sensing techniques for electrochemical detection of biomarkers, mainly UA and DA, with the main emphasis on derivatives of graphene. In the first section of the article, graphene-based materials that have been recently used for the development of electrochemical sensors of DA and UA are discussed. This will include graphene oxide (GO), graphene quantum dots (GQD) and reduced graphene oxide (RGO). Subsequently, several surface modification approaches and major factors



Scheme I. Typical configurations of N atoms in graphene: **A** pyridinic-N; **B** graphitic-N; **C** triple vacancy pyridinic-N; **D** pyrrolic-N and **E** oxidised pyridinic-N (NOx). (Reproduced with permission (41). Copyright © 2016 the Royal Society of Chemistry)

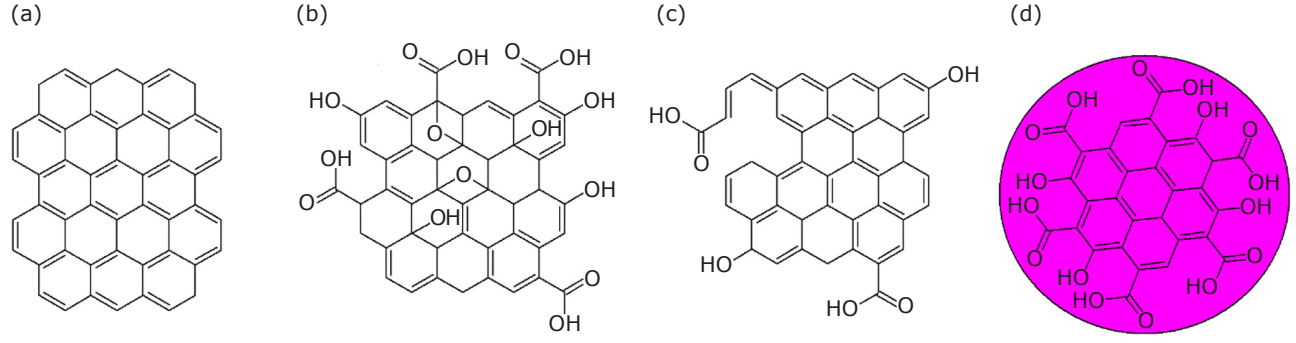
© 2019 Johnson Matthey

that influence or enhance the sensing performance of these graphene-based DA/UA sensors will be reviewed. The main focus of the last section will be on the variations of the electrocatalytic performances of recent up-to-date graphene-based sensors, as conferred by the introduction of p-block heteroatoms, with special emphasis on N dopants.

2. Graphene-Based Materials for Detection of Dopamine and Uric Acid

Graphene, an allotrope of carbon with a 2D structure and the first example of a free-standing and stable 2D material, has attracted enormous research interest in science communities (39, 40, 49). The large electrical conductivity, surface area, high tensile strength and thermal properties make graphene a promising and ideal candidate material for application in fields such as nanomaterials, supercapacitors, nanoelectronics, catalysis, nanophotonics and sensors (39–40, 47–49). Recently, graphene derivatives have been intensively employed as modification materials on the surface of different electrodes for detection of various analytes (28–30, 50). However, the usefulness of different graphene derivatives for engineering selective, sensitive and stable electrochemical biosensors is in large part dependent on their structure. This is because the morphological and intrinsic properties of various graphene moieties control the limit of detection (LOD), sensitivity, selectivity, repeatability and biocompatibility of any graphene-based electrochemical biosensors. **Scheme II** shows some of the major graphene derivatives, pristine (**Scheme II(a)**) and functionalised (**Scheme II(b)–(d)**), that have recently been intensively employed to modify different electrodes for detection of various analytes (28–30, 50). It can be seen that the structure of pristine graphene is characterised by an array of sp^2-hybridised carbon atoms arranged in a 2D hexagonal lattice (39, 40, 49). The carbon backbone can be oxidised to form GO (51, 52) or the oxygen functionalities can be removed *via* the use of chemical, electrical or thermal procedures to form a defect-filled structure of RGO (53, 54). On the other hand, different preparation methods can be adopted to synthesise few nanometre-sized graphene moieties known as GQD, due to their quantum properties (55, 56). Owing to the photoluminescence properties of GQDs, these derivatives of graphene have found application in the field of optochemical biosensors (57, 58).

The majority of graphene-based electrochemical sensors for DA and UA are fabricated from suspensions and powders of different types of GO derivatives such as thermally reduced graphene oxide (TRGO), electrochemically reduced graphene oxide (ERGO), hydrothermally prepared multi-nanoporous graphene and chemically reduced graphene oxide (CRGO) (59–63). For instance, Wang and coworkers as well as Zhu *et al.* reported on the fabrication of porous graphene provided channels that accelerated the diffusion of the electrolyte and promoted the mass transfer process (59, 60). They observed that the large accessible surface area and the highly conductive channels, due to the presence of abundant carboxylic or hydroxide groups, edges and defective sites, remarkably enhanced the electrocatalytic performance and selectivity of this three-dimensional (3D) graphene modified glassy carbon electrode (GCE) for the simultaneous detection of DA and UA. However, the use of corrosive chemicals during the synthesis steps of the porous graphene led to loss of the surface area as well as a lowered degree of reduction (11, 59).



Scheme II. Structures of graphene derivatives: (a) the pristine graphene; (b) graphene oxide (GO); (c) reduced graphene oxide (RGO) and (d) graphene quantum dot (GQD)

© 2019 Johnson Matthey

Thus, reports have shown that the issues associated with a lowered surface area could be solved by using RGO. In particular, Yang *et al.* as well as Yu *et al.* indicated that the oxygenated species and absorption sites of the ERGO catalysed the electrochemical oxidation reactions of DA, UA and AA (61, 62). Apart from the use of electrochemical procedures to obtain RGO nanomaterials, Kanyong *et al.* successfully fabricated in-house disposable screen printed carbon electrodes modified with CRGO nanosheets which showed excellent electrocatalytic performance towards DA, UA and AA (63). Moreover, Wang and coworkers attributed the high electrocatalytic activity of the RGO-based glassy electrodes, in terms of a wide linear range and low detection limits for DA, UA and AA, to the abundance of edges and defective sites on the wrinkles and plane sites (64). As a result, these greatly enhanced the electron transfer activity between the molecules and graphene and also increased the surface area for adsorption of these electroactive molecules. Electroanalytical data for the selective determination of DA and UA by use of electrodes modified with various graphene derivatives are listed in **Table I** (11, 59–65). An informative review on the applications of graphene for electrochemical sensing and biosensing was recently published by Pumera *et al.* (33, 34).

Although the abovementioned derivatives of graphene have shown excellent electrocatalytic activity towards DA, UA and AA at various conventional working electrodes, tedious and irreproducible pretreatment steps are frequently required to immobilise the as-synthesised powdered graphene on the electrode surface. This is achieved by using specialised electrode surface modification techniques, such as surface coating of conventional electrodes or generation of a carbon paste with surfactants and binders like sodium dodecyl sulphate (SDS), dihexadecyl phosphate (DHP) and Nafion™, in order to immobilise the graphene nanomaterials on the electrodes (66–71). Furthermore, the aggregation of the graphene nanosheets during electrode preparation led to loss of electrocatalytic activity towards the oxidation of biomolecules (8, 10). Thus a protocol for the fabrication of surfactant-free graphene-based biosensors is needed and this was illustrated in our previous studies (65). In the study, chemical vapour deposition (CVD) grown graphene films were used as a modifying material for the indium tin oxide (ITO) electrode for the detection of DA and UA (**Figure 1**). The choice of the working electrode was based on the fact that the ITO electrodes are less commonly used as electrochemical electrode materials (72, 73), although they have profound application in energy storage and energy devices (38, 40, 74, 75). We found that under optimised differential pulse voltammetry (DPV) conditions, Gr/ITO electrode exhibited wide linear ranges, fairly reasonable stability and reproducibility, as well as good selectivity for both DA and UA. However, the Gr/ITO suffered poor sensitivity and high detection limits (S:N = 3) for DA and UA, with the limits of detection determined to be 4.23 μM and 5.94 μM, respectively. The promising electrocatalytic performance was ascribed to the 'flat' 2D structure of the graphene films due to the abundance of surface carbon atoms available for electron transfer with both DA and UA. Thus, the results showed that with further improvements such as control of the defect density and the thickness of the graphene films, Gr/ITO electrodes are promising candidates for simultaneous determination of DA and UA.

Table I Electroanalytical Parameters for the Detection of DA and UA at Various Electrodes Modified with Graphene Derivatives

Electrode [a]	Detection limit, μM		Linear range, μM		Ref.
	DA	UA	DA	UA	
PGE/GCE	0.2	1	0.2–8	1–60	(59)
3D-GrF/GCE	0.025	–	0.1–25	–	(60)
ERGO/GCE	0.5	0.5	0.5–60	0.5–60	(61)
3D-RGO/GCE	5	–	5–1000	–	(11)
ERGO/GCE	0.1	–	0.1–10	–	(62)
RGO/SPCE	0.4	0.1	120–500	10–3000	(63)
RGO/GCE	0.1	1	0.1–400	2–600	(64)
Gr/ITO	4.1	5.9	8–190	40–560	(65)

[a] Porous graphene electrode (PGE); screen printed carbon electrode (SPCE); graphene foam (GrF)

© 2019 Johnson Matthey

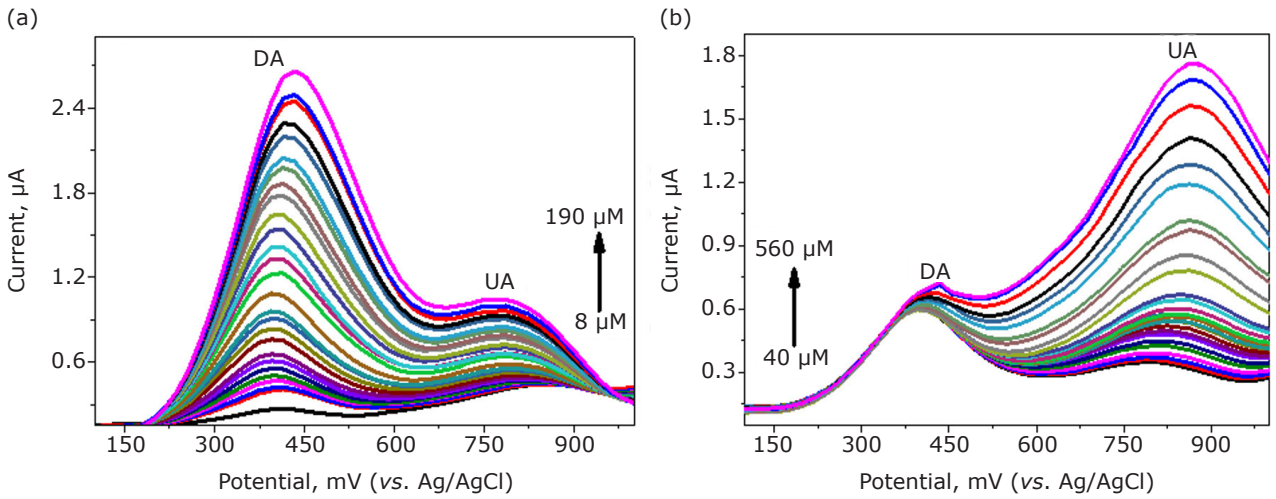


Fig. 1. DPV curves for a system containing; (a) fixed concentrations of UA (10 μM) and different concentrations of DA; (b) fixed concentrations of DA (10 μM) and different concentrations of UA on Gr/ITO electrodes at 0.1 M buffer pH 6.02 (65)

3. Surface Modification Approaches for Graphene-Based Electrodes for Dopamine and Uric Acid

The structural and remarkable properties of different derivatives of graphene have rendered them promising and potential candidates for successful exploitation in electrochemical and biosensing applications. As sensitive and selective as the graphene derivatives have proved to be for the electrochemical sensing of biomarkers such as DA and UA, a great deal of research effort has been devoted to further improving the structural and intrinsic properties of graphene in order to engineer high-performance graphene-based electrochemical sensors that stand a chance to compete with their metal or metal oxide-based counterparts. As such, a variety of surface modification approaches have been explored, including introduction of heteroatoms into the graphene lattice (48, 76, 77) or formation of composite materials of graphene with other carbon nanostructures, polymeric materials, as well as metal and metal oxides (78–85). This is because surface modification increases the surface-area-to-volume ratio of the graphene-based electrode; therefore the signal transduction can be amplified, leading to higher sensitivity compared to the conventional sensing surfaces. Thus, this section reviews the recent surface modification techniques used for the fabrication of graphene-based electrochemical sensors for DA and UA, with the focus on highlighting the design of surfactant-free graphene-based electrodes for DA and UA.

3.1 Graphene Composite-Based Electrodes for Dopamine and Uric Acid

Lately, numerous modified electrodes based on different graphene derivatives have been successfully employed for the electrochemical detection of DA, UA and many other electrochemically active biomarkers. Such electrodes include, but are not limited to the modification of conventional electrodes with GO-metal oxide or GO-carbon nanomaterial composite, GO-bimetallic nanoclusters and GO-polymer nanosheets (78–85). For instance, fabrication of sensors based on nanocomposites of GO and polymers such as poly-*L*-lysine (PLL) has gained increasing interest due to their good biocompatibility with amino acids as well as their flexible structure framework. As a result, numerous chemically stable and highly sensitive and selective sensors have been fabricated based on GO-PLL nanocomposites for the detection of DA, UA, AA, glucose and hydrogen peroxide (H_2O_2) (78–82). The excellent electrocatalytic performance of the electrodes is largely ascribed to the excellent synergistic effect of the two materials for adsorption of electroactive (bio) molecules. Apart from the use of biocompatible polymers, Zhang *et al.* illustrated that modification of the ITO electrode with a composite of RGO and carbon nanotubes (CNTs) enhanced the sensing performance of ITO electrodes for the simultaneous detection of DA, UA and AA (78). This was attributed to the excellent performance due to the high electrocatalytic activity of RGO,

 © 2019 Johnson Matthey

the combined large accessible surface area of both RGO and CNTs, as well as the presence of highly conductive channels of the CNTs which facilitated a faster mass transfer process.

On the other hand, various reports indicated that inclusion of the catalytic metal nanoparticles on the surface of the working electrode can also enhance the performance of the graphene-based chemical sensors (65, 80–85). Metal and metal oxide nanoparticles are the most widely used catalysts because of their unique chemical, electrical and catalytic properties. Therefore, the presence of the metal nanoparticles on the graphene-modified electrode surface greatly increases the overall sensing surface area, facilitates faster electron transfer rate for electrocatalytic oxidation, thus leading to a sensitive and selective signal response. For instance, Zhang and coworkers reported that the excellent synergistic effect between GO and gold nanoparticles as well as the combined high electrical conductivity of gold nanoparticles and the ITO electrode led to high performance sensors of DA (80). In addition, He *et al.* showed that combining the good catalytic activity of copper oxide (Cu_2O) nanoparticles with the excellent dispersion ability of reduced graphene, led to a facile fabrication of a sensor exhibiting rapid response, a low detection limit and a wide linear range for simultaneous detection of DA, AA and UA (85). As a result, numerous reports have shown that fabricating a composite of the graphene derivatives with either metal oxide or bimetallic nanoparticles enhanced the sensitivity and improved the selectivity of such electrodes for the simultaneous detection of DA, UA and various analytes (83–92). The excellent electrocatalytic performance was also attributed to the synergistic effect between graphene derivative and the nanoparticles. Specifically, in terms of the ability of graphene to facilitate good dispersion of the nanoparticles, the presence of abundant oxygen functionalities for improved π-π interaction between the molecules and the edge- and plane-like binding sites on the electrode surface, as well as the high electrical conductivity of catalyst nanoparticles. Thus, incorporation of metal nanoparticles has proven to greatly improve the electrocatalytic activity of the graphene-based sensors for DA and UA. However, pre-treatment procedures such as surface coating or generation of a carbon paste with surfactants and binders like SDS, DHP and Nafion™, are mandatory in order to immobilise the graphene/nanoparticle composites on the electrodes (66–71). Secondly, leaching of the metal nanoparticles into the electrode, if not immobilised carefully, constitute one of the major drawbacks of the promising potential application of electrochemical sensors based on graphene-metal composites. Moreover, electrode surface modification with graphene/nanoparticle composites may result in an increase in background noise and faster electrode fouling due to chemical reactions which can occur between the nanoparticles and surfactants or binders.

To circumvent this issue, we proposed a protocol for fabricating surfactant-free graphene/nanoparticle-based electrochemical sensors for detection of DA and UA (65). By using an electroless deposition procedure, platinum and palladium nanoparticles were supported on CVD-grown graphene films. Thereafter, the graphene/nanoparticle composites were used as modifying material for the ITO electrode for the detection of DA and UA (**Figure 2**). Regardless of the different binding behaviours of Pt and Pd on the surface of graphene, with Pt showing a weak physisorption binding energy of <0.5 eV and Pd demonstrating a strong chemisorption binding energy of >0.8 eV (42), the electrochemical performances and stability of these composite-based ITO electrodes were also found to be dependent on the sizes of the metal nanoparticles, as reported in literature (65, 83–85). For instance, modification of the graphene films with small Pt nanoparticles (5 ± 3 nm) enhanced the sensitivity of these electrodes for DA and UA, in comparison to their pristine counterparts and graphene films modified with large Pd nanoparticles (22 ± 7 nm). As this was a pioneering study for the use of electroless deposition of metal nanoparticles on CVD-grown graphene films for electrochemical detection of DA and UA, we propose that more studies should be performed in order to investigate the influence of same-sized Pt and Pd nanoparticles as well as the intentionally controlled structural and electronic properties of graphene films for the detection of DA and UA.

3.2 P-Block Element Doped Graphene-Based Electrodes for Dopamine and Uric Acid

Incorporation of p-block elements, such as nitrogen, boron, hydrogen, oxygen, sulfur and fluorine, is currently one of the promising procedures for intentional tailoring of the electronic and electrochemical properties of graphene (41, 44–46). Doping is also an effective way to modify the local chemical activity of graphene derivatives,

 © 2019 Johnson Matthey

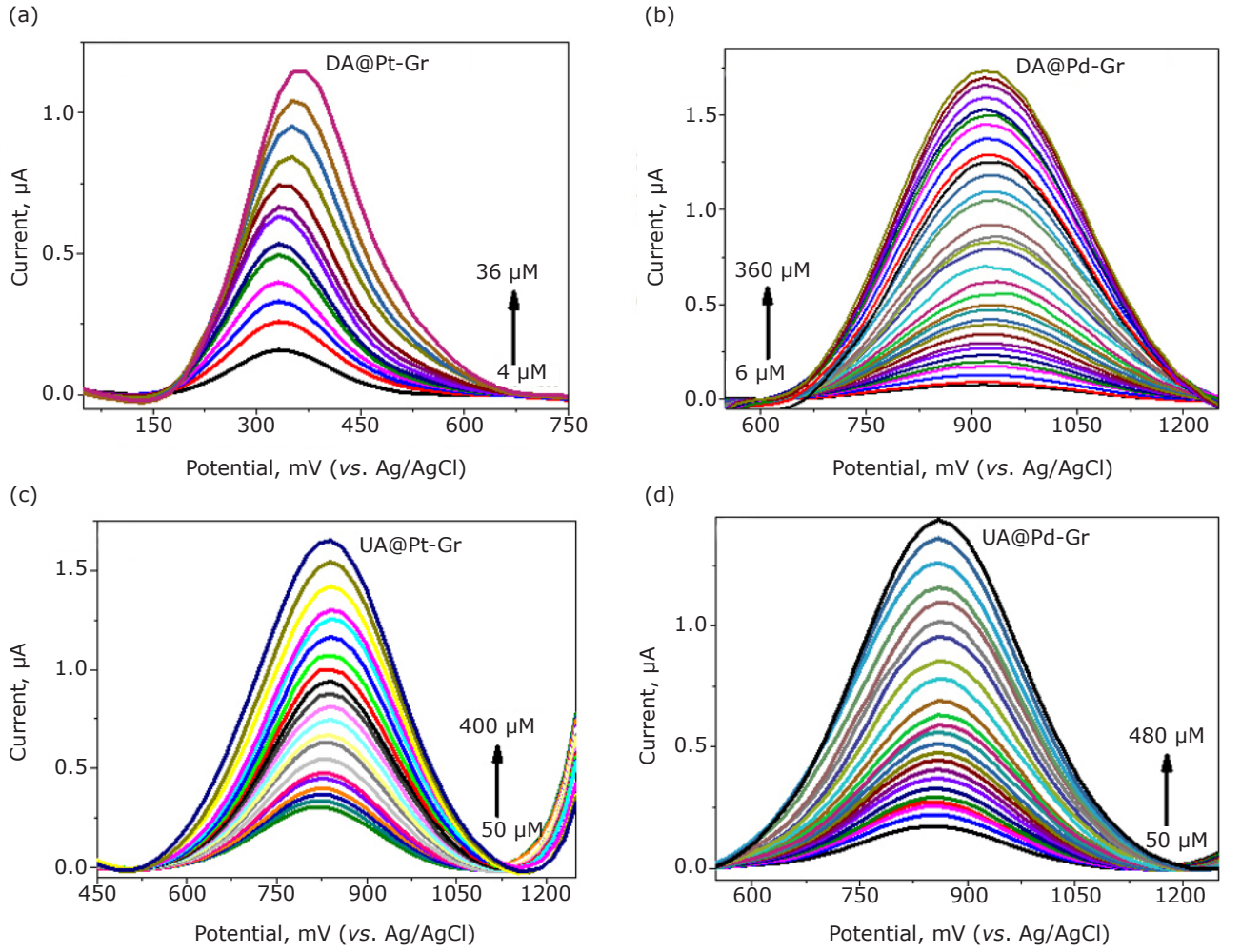


Fig. 2. DPV curves for a 0.1 M buffer solution (pH 6.02) containing: (a) 0.13 mM DA at Pt-Gr/ITO electrodes; (b) 0.13 mM DA at Pd-Gr/ITO electrodes (c) 0.13 mM UA at Pt-Gr/ITO electrodes; (d) 0.13 mM UA at Pd-Gr/ITO electrodes (71)

subsequently widening their application in various technological devices (40, 93, 94). Among the various dopants, N is the most widely used for improving the performance of graphene-based electrochemical sensors (42–46) due to its comparative atomic size (d_N = 70 pm *vs*. d_C = 65 pm) and the extra electron in its outer shell. For example, Brownson *et al.* showed that GCE modified NGr nanosheets exhibited an enhanced electrocatalytic activity towards the oxidation of AA, DA and UA in comparison with the bare and the undoped graphene modified GCE (48). Han *et al.* reported that modification of the GCE with chitosan-functionalised graphene showed excellent sensitivity and selectivity towards the electrocatalytic oxidation of DA, UA and AA (42). These research reports and many more in the literature highlight that the enhanced biocompatibility and sensitivity of NGr in electrochemical sensors can be attributed to the presence of N atoms which provide a large amount of edge- and plane-like binding sites for biomolecules (7, 11–15, 28). This can be attributed to the various ways in which N atoms become incorporated into the graphene lattice (**Scheme I**) (41), thus providing abundant binding sites for adsorption of DA and other electroactive biomolecules (47, 48). Even though the successful application of the powdered N-doped derivatives of graphene, as well as other N-doped carbon nanomaterials, in electrochemical sensors has been reported by various research groups, little attention has been paid to the influence and contribution of the content of each N-configuration on the electrocatalytic activity of N-graphene nanosheets towards the oxidation of biomolecules such as DA.

As such, using large-area N-doped graphene films with well controlled N-configurations (41), we developed a platform for studying the influence of the content of each N-configuration on the inherent

 © 2019 Johnson Matthey

electrocatalytic activity of the N-graphene films towards the oxidation of DA and UA, in the presence of their common interfering agents (95, 96). From **Figure 3**, the electrochemical responses of DA, UA and AA at the different modified NGr/ITO electrode surfaces are observed to vary due to the different interactions of the electroactive molecule with the N-configurations on the NGr/ITO electrode surface. For example, all NGr/ITO electrodes showed enhanced voltammetric responses for DA and UA, suggesting improved sensitivity. Conversely, the low voltammetric responses of AA at all NGr/ITO electrodes are due to the electrostatic repulsion of negatively charged AA molecules (pKa = 4.1) from the electron-rich NGr-electrode surface. Generally, the good selectivity and sensitivity of NGr-2/ITO electrodes were attributed to the good interaction between the hydroxyl and amine groups on the DA and UA and the defective N binding sites (NOx, pyrrolic-N).

Comparison of the electroanalytical parameters of our fabricated NGr/ITO electrodes with the reported N-doped carbon-based electrodes (**Table III**), indicated that modification of the surface chemistry of the 2D NGr films supported on the ITO electrodes, *via* control of the content of the N-configurations, led to the development of electrochemical sensors exhibiting comparable or better electrochemical performance (7, 95–100). In particular, the electrochemical performance for DA and UA at all NGr/ITO electrodes was dependent on the presence of defective N-configurations, especially pyrrolic-N and NOx, whereas relatively high concentrations of graphitic-N configurations hindered the electron transfer. This was facilitated through increased hydrogen bonding and improved π-π interaction between DA and the carbon surface (74, 97–99). Most importantly, the structure of the electroactive molecule was also found to be the major determining factor for electrochemical

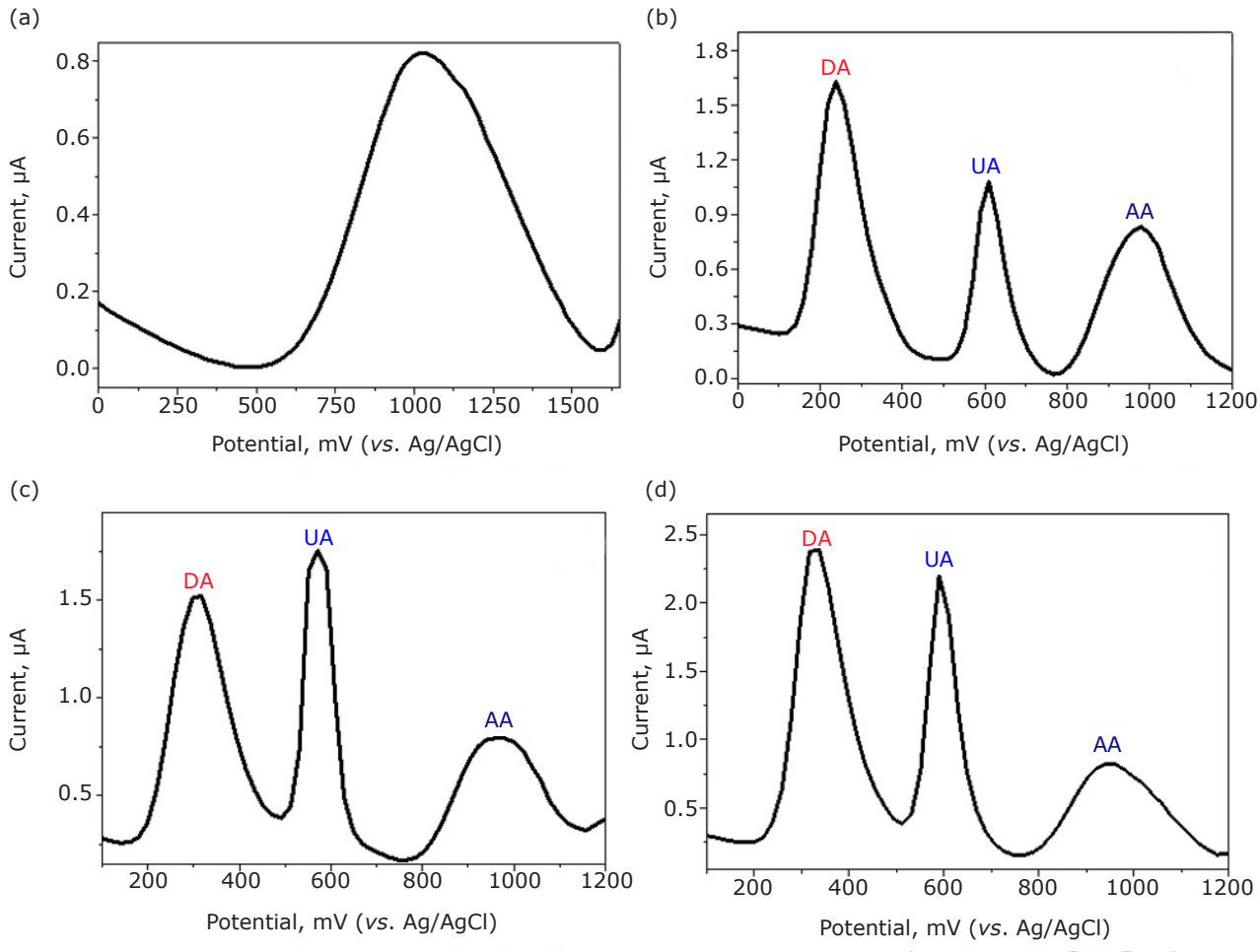


Fig. 3. DPV curves of the electrochemical oxidation of 20 μM DA, 100 μM UA and 200 μM AA at: (a) bare ITO; (b) NGr-2/ITO; (c) NGr-10/ITO; (d) NGr-20/ITO electrodes (Reprinted from (95), copyright (2018), with permission from Elsevier)

© 2019 Johnson Matthey

Table II Electroanalytical Parameters for the Detection of DA and UA at Various Electrodes Modified with Graphene Composites

Electrode [a]	Detection limit, μM		Linear range, μM		Ref.
	DA	UA	DA	UA	
PLL-GO/GCE	0.031	–	0.5–20	–	(78)
RGO-CNT/ITO	0.04	0.17	0.2–8	0.2–16	(79)
Au-GO/ITO	0.06	–	10–1000	–	(80)
Pt-Gr/ITO	0.29	0.34	4–36	50–400	(65)
Pd-Gr/ITO	0.76	0.47	6–360	50–480	(65)
Pd_3Pt_1-PDDA-RGO/GCE	0.04	0.1	4–20	4–400	(83)
Fe_3O_4@Au-S-Fc/ GS-chit	0.15	0.24	0.5–50	1–300	(84)
Cu_2O/RGO/GCE	0.006	–	0.08–50	–	(85)
Pt-Ni/PDA/RGO/GCE	0.07	–	0.2–911	–	(86)
MnO_2NR/RGO/GCE	–	0.01		0.05–400	(87)
RGO-poly(Cu-AMT)/GCE	0.004	–	0.01–40	–	(88)
Au-Pt/GO-ERGO/GCE	0.0207	0.0407	0.07–49800	0.13–83000	(89)
MgO/Gr/Ta/GCE	0.1–7	1–70	0.15	0.12	(90)

[a] Gold nanoparticles (Au); platinum nanoparticles (Pt); palladium nanoparticles (Pd); poly(diallyldimethylammonium) chloride (PDDA); GO nanosheets (GO); ferric oxide (Fe_3O_4); graphene sheet (GS); ferrocene thiolate (S-Fc); chitosan (chit); poly(dopamine) (PDA); nickel nanoparticles (Ni); copper oxide nanoparticles (Cu_2O); manganese oxide nanoribbons (MnO_2NR); polymerised copper-2-amino-5-mercapto-1,3,4 thiadiazole complex (poly(Cu-AMT)); ERGO nanosheets (ERGO); magnesium oxide nanobelts (MgO); tantalum wire (Ta)

Table III Electroanalytical Parameters for the Detection of DA and UA at Various Electrodes Modified with N-Graphene Derivatives

Electrode [a]	N-configuration	Detection limit, μM		Linear range, μM		N:C, %	Ref.
		DA	UA	DA	UA		
NGr-2/ITO	pyrrolic, pyridinic	0.13	0.043	2–240	2–320	4.68	(95, 96)
NGr-10/ITO	graphitic, pyridinic	0.15	0.19	2–150	20–140	3.25	(95, 96)
NGr-20/ITO	pyridinic	0.65	0.096	4–40	6–200	2.84	(95, 96)
3D-NHPC/GCE	pyrrolic	0.020	0.14	0.05–14.5	2–30	2.01	(97)
NCNF/GCE	pyridinic, pyrrolic	0.5	0.992	1–10	5–2000	–	(98)
NGO/GCE	pyridinic, pyrrolic	0.25	0.45	0.5–170	0.1–200	–	(7)
MNC/GCE	pyridinic, pyrrolic	0.001	0.01	0.001–30	0.01–30	12.2	(100)
NHCS/GCE	graphitic, pyridinic	0.30	0.52	1–400	1–420	–	(99)

[a] N-doped graphene film (NGr); N-doped RGO nanosheets (NGO); N-doped graphene fibres (NGF); N-doped hierarchically porous carbon (NHPC); mesoporous N-doped carbon (MNC); N-doped hollow carbon spheres (NHCS); N-doped carbon nanofibers (NCNF)

performance of differently N-doped graphene electrodes.

4. Conclusions

In this article, we have illustrated that, although research on graphene-based electrochemical sensors for DA and UA started almost a decade ago, a great deal of effort has been devoted to improving the electrochemical performance of these sensors. In our previous studies, we demonstrated a new strategy of designing surfactant-free electrochemical sensors for the selective and sensitive detection of DA and UA in the presence of interfering agents. This new strategy is based on the modification of ITO electrodes with differently N-doped graphene films. The study indicated a good correlation between the relative concentrations of different N-configurations of N-doped graphene films with the electrocatalytic activity of the NGr/ITO electrodes towards the oxidation of DA and UA. Therefore, by combining the highly conductive 2D structure of graphene with the excellent conducting properties of ITO electrodes and a careful control

 © 2019 Johnson Matthey

of the N-configurations, a satisfactory performance for the electrocatalytic oxidation of DA and UA in the presence of high concentrations of their most common interfering agents was established for NGr/ITO-based electrodes. Finally, the study indicated that, not only should the correlation between the N-configurations and the electrochemical performance of N-graphene-based electrodes be considered, but also the structure of the electroactive molecule of interest must be taken into serious consideration for the development of satisfactory N-graphene based electrochemical sensors.

Glossary

AA	ascorbic acid
chit	chitosan
CNT	carbon nanotube
CRGO	chemically reduced graphene oxide
DA	dopamine
ERGO	electrochemically reduced graphene oxide
GCE	glassy carbon electrode
GO	graphene oxide
GQD	graphene quantum dots
GrF	graphene foam
GS	graphene sheet
ITO	indium tin oxide
MNC	mesoporous N doped carbon
MnO_2NR	manganese oxide nanoribbons
NCNF	N doped carbon nanofibers
NGF	N doped graphene fibres
NGr	nitrogen-doped graphene
NHCS	N doped hollow carbon spheres
NHPC	N doped hierarchically porous carbon
PDC	polymer derived ceramics
PDA	poly(dopamine)
PDDA	poly(diallyldimethylammonium) chloride
PGE	porous graphene electrode
PLL	poly-*L*-lysine
poly(Cu-AMT)	polymerised copper-2-amino-5-mercapto-1,3,4 thiadiazole complex
RGO	reduced graphene oxide
S-Fc	ferrocene thiolate
SPCE	screen printed carbon electrode
TRGO	thermally reduced graphene oxide
UA	uric acid

Acknowledgements

The authors thank Johnson Matthey, Pretoria, South Africa; the University of the Witwatersrand, South Africa, Postgraduate Merit Award; the DST-NRF Centre of Excellence in Strong Materials (CoESM), South Africa; and the NRF, South Africa, for financial support.

References

1. H.-W. Wang, Y.-H. Wei and H.-W. Guo, *Anticancer Agents Med. Chem.*, 2009, **9**, (9), 1012
2. J. Li and X. Lin, *Sensors Actuators B: Chem.*, 2007, **124**, (2), 486
3. A. J. Bard and L. R. Faulker, "Electrochemical Methods: Fundamentals and Applications", 2nd Edn., John Wiley and Sons Inc, New York, USA, 2001
4. Z. Wang, S. Liu, P. Wu and C. Cai, *Anal. Chem.*, 2009, **81**, (4), 1638
5. D. M. Anjo, M. Kahr, M. M. Khodabakhsh, S. Nowinski and M. Wanger, *Anal. Chem.*, 1989, **61**, (23), 2603
6. H. Xu, J. Xiao, L. Yan, L. Zhu and B. Liu, *J. Electroanal. Chem.*, 2016, **779**, 92
7. Z.-H. Sheng, X.-Q. Zheng, J.-Y. Xu, W.-J. Bao, F.-B. Wang and X.-H. Xia, *Biosens. Bioelectron.*, 2012, **34**, (1), 125
8. P. K. Aneesh, S. R. Nambiar, T. P. Rao and A. Ajayaghosh, *Anal. Methods*, 2014, **6**, (14), 5322
9. L. Wang, P. Huang, J. Bai, H. Wang, X. Wu and Y. Zhao, *Int. J. Electrochem. Sci*., 2006, **1**, (6), 334
10. G. Liu, W. Ma, Y. Luo, D. Sun and S. Shao, *J. Anal. Methods Chem.*, 2014, 984314
11. Y.-R. Kim, S. Bong, Y.-J. Kang, Y. Yang, R. K. Mahajan, J. S. Kim and H. Kim, *Biosens. Bioelectron.*, 2010, **25**, (10), 2366
12. S. Qi, B. Zhao, H. Tang and X. Jiang, *Electrochim. Acta*, 2015, **161**, 395
13. K. Jackowska and P. Krysinski, *Anal. Bioanal. Chem.*, 2013, **405**, (11), 3753
14. L. M. Niu, K. Q. Lian, H. M. Shi, Y. B. Wu, W. J. Kang and S. Y. Bi, *Sensors Actuators B: Chem.*, 2013, **178**, 10
15. M. Sajid, M. K. Nazal, M. Mansha, A. Alsharaa, S. M. S. Jillani and C. Basheer, *TrAC Trends Anal. Chem.*, 2016, **76**, 15

 © 2019 Johnson Matthey

16. A. Gottås, Å. Ripel, F. Boix, V. Vindenes, J. Mørland and E. L. Øiestad, *J. Pharmacol. Toxicol. Methods*, 2015, **74**, 75
17. S. B. Floresco, A. R. West, B. Ash, H. Moore and A. A. Grace, *Nat. Neurosci.*, 2003, **6**, (9), 968
18. I. Sano, T. Gamo, Y. Kakimoto, K. Taniguchi, M. Takesada and K. Nishinuma, *Biochim. Biophys. Acta*, 1959, **32**, 586
19. R. M. Wightman, L. J. May and A. C. Michael, *Anal. Chem.*, 1988, **60**, (13), 769A
20. S. Kapur and D. Mamo, *Prog. Neuro-Psychopharmacol. Biol. Psychiatry*, 2003, **27**, (7), 1081
21. "Handbook of the Neuroscience of Aging", eds. C. V. Mobbs and P. R. Hof, Elsevier Inc, London, UK, 2009
22. M. Mazzali, J. Hughes, Y.-G. Kim, J. A. Jefferson, D.-H. Kang, K. L. Gordon, H. Y. Lan, S. Kivlighn and R. J. Johnson, *Hypertension*, 2001, **38**, (5), 1101
23. R. Gowrishankar, M. K. Hahn and R. D. Blakely, *Neurochem. Int.*, 2014, **73**, 42
24. K. A. Montagu, *Nature*, 1957, **180**, (4579), 244
25. V. V. S. Eswara Dutt and H. A. Mottola, *Anal. Chem.*, 1974, **46**, (12), 1777
26. S. Liu, X. Xing, J. Yu, W. Lian, J. Li, M. Cui and J. Huang, *Biosens. Bioelectron.*, 2012, **36**, (1), 186
27. X. Chen, G. Wu, Z. Cai, M. Oyama and X. Chen, *Microchim. Acta*, 2014, **181**, (7–8), 689
28. J. Yu, S. Wang, L. Ge and S. Ge, *Biosens. Bioelectron.*, 2011, **26**, (7), 3284
29. H. Sun, J. Chao, X. Zuo, S. Su, X. Liu, L. Yuwen, C. Fan and L. Wang, *RSC Adv.*, 2014, **4**, (52), 27625
30. L. Wang, X. Lu, C. Wen, Y. Xie, L. Miao, S. Chen, H. Li, P. Li and Y. Song, *J. Mater. Chem. A*, 2015, **3**, (2), 608
31. P. Shakkthivel and S.-M. Chen, *Biosens. Bioelectron.*, 2007, **22**, (8), 1680
32. S. Cinti, F. Arduini, M. Carbone, L. Sansone, I. Cacciotti, D. Moscone and G. Palleschi, *Electroanal.*, 2015, **27**, (9), 2230
33. A. Ambrosi, C. K. Chua, A. Bonanni and M. Pumera, *Chem. Rev.*, 2014, **114**, (14), 7150
34. A. Ambrosi, C. K. Chua, N. M. Latiff, A. H. Loo, C. H. A. Wong, A. Y. S. Eng, A. Bonanni and M. Pumera, *Chem. Soc. Rev.*, 2016, **45**, (9), 2458
35. M. Pumera, B. Šmíd and K. Veltruská, *J. Nanosci. Nanotechnol.*, 2009, **9**, (4), 2671
36. A. A. Abdelwahab and Y.-B. Shim, *Sensors Actuators B: Chem.*, 2015, **221**, 659
37. S. Komathi, A. I. Gopalan and K.-P. Lee, *Analyst*, 2010, **135**, (2), 397
38. S. Cheemalapati, S. Palanisamy, V. Mani and S.-M. Chen, *Talanta*, 2013, **117**, 297
39. A. K. Geim and K. S. Novoselov, *Nature Mater.*, 2007, **6**, (3), 183
40. K. S. Novoselov, A. K. Geim, S. V. Morosov, D. Jiang, Y. Zhang, S. V. Dubonos, I. V. Grigorieva and A. A. Firsov, *Science*, 2004, **306**, (5696), 666
41. B. J. Matsoso, K. Ranganathan, B. K. Mutuma, T. Lerotholi, G. Jones and N. J. Coville, *RSC Adv.*, 2016, **6**, (108), 106914
42. D. Han, T. Han, C. Shan, A. Ivaska and L. Niu, *Electroanal.*, 2010, **22**, (17–18), 2001
43. X. Dong, D. Fu, W. Fang, Y. Shi, P. Chen and L.-J. Li, *Small*, 2009, **5**, (12), 1422
44. R. Lv and M. Terrones, *Mater. Lett.*, 2012, **78**, 209
45. C.-K. Chang, S. Kataria, C.-C. Kuo, A. Ganguly, B.-Y. Wang, J.-Y. Hwang, K.-J. Huang, W.-H. Yang, S.-B. Wang, C.-H. Chuang, M. Chen, C.-I. Huang, W.-F. Pong, K.-J. Song, S.-J. Chang, J.-H. Guo, Y. Tai, M. Tsujimoto, S. Isoda, C.-W. Chen, L.-C. Chen and K.-H. Chen, *ACS Nano*, 2013, **7**, (2), 1333
46. P. P. Shinde and V. Kumar, *Phys. Rev. B*, 2011, **84**, (12), 125401
47. M. Pumera, A. Ambrosi, A. Bonanni, E. L. K. Chng and H. L. Poh, *TrAC Trends Anal. Chem.*, 2010, **29**, (9), 954
48. D. A. C. Brownson, D. K. Kampouris and C. E. Banks, *Chem. Soc. Rev.*, 2012, **41**, (21), 6944
49. K. S. Novoselov, A. K. Geim, S. V Morozov, D. Jiang, M. I. Katsnelson, I. V. Grigorieva, S. V. Dubonos and A. A. Firsov, *Nature*, 2005, **438**, (7065), 197
50. C. Zhang, Z. Zhang, Q. Yang and W. Chen, *Electroanal*., 2018, **30**, (11), 2504
51. W. S. Hummers and R. E. Offeman, *J. Am. Chem. Soc.*, 1958, **80**, (6), 1339
52. N. I. Zaaba, K. L. Foo, U. Hashim, S. J. Tan, W.-W. Liu and C. H. Voon, *Procedia Eng.*, 2017, **184**, 469
53. S. Stankovich, D. A. Dikin, R. D. Piner, K. A. Kohlhaas, A. Kleinhammes, Y. Jia, Y. Wu, S. T. Nguyen and R. S. Ruoff, *Carbon*, 2007, **45**, (7), 1558
54. H. A. Becerril, J. Mao, Z. Liu, R. M. Stoltenberg, Z. Bao and Y. Chen, *ACS Nano*, 2008, **2**, (3), 463
55. S. Bak, D. Kim and H. Lee, *Curr. Appl. Phys.*, 2016, **16**, (9), 1192
56. L. A. Ponomarenko, F. Schedin, M. I. Katsnelson, R. Yang, E. W. Hill, K. S. Novoselov and A. K. Geim, *Science*, 2008, **320**, (5874), 356
57. L. Wang, W. Li, B. Wu, Z. Li, S. Wang, Y. Liu, D. Pan and M. Wu, *Chem. Eng. J.*, 2016, **300**, 75
58. M. Hassan, E. Haque, K. R. Reddy, A. I. Minett, J. Chen and V. G. Gomes, *Nanoscale*, 2014, **6**, (20), 11988

 © 2019 Johnson Matthey

59. Y. Wang, Y. Huang, B. Wang, T. Fang, J. Chen and C. Liang, *J. Electroanal. Chem.*, 2016, **782**, 76
60. X. Dong, X. Wang, L. Wang, H. Song, H. Zhang, W. Huang and P. Chen, *ACS Appl. Mater. Interfaces*, 2012, **4**, (6), 3129
61. L. Yang, D. Liu, J. Huang and T. You, *Sensors Actuators B: Chem.*, 2014, **193**, 166
62. X. Yu, K. Sheng and G. Shi, *Analyst*, 2014, **139**, (18), 4525
63. P. Kanyong, S. Rawlinson and J. Davis, *Chemosens.*, 2016, **4**, (4), 25
64. H. Wang, F. Ren, C. Wang, B. Yang, D. Bin, K. Zhang and Y. Du, *RSC Adv.*, 2014, **4**, (51), 26895
65. B. J. Matsoso, T. Lerotholi, G. Jones and N. J. Coville, 'CVD Growth of Pristine and N-Doped Graphene Films for Support of Platinum and Palladium Nanoparticles in Electrochemical Sensing of Dopamine and Uric Acid', PhD Thesis, University of the Witwatersrand, Johannesburg, South Africa, 2017, pp. 96–131
66. J. G. Manjunatha, B. E. Kumara Swamy, G. P. Mamatha, U. Chandra, E. Niranjana and B. S. Sherigara, *Int. J. Electrochem. Sci*., 2009, **4**, (2), 187
67. J. Oni and T. Nyokong, *Anal. Chim. Acta*, 2001, **434**, (1), 9
68. J. F. Rusling, *Acc. Chem. Res.*, 1991, **24**, (3), 75
69. Y. Sun, J. Fei, K. Wu and S. Hu, *Anal. Bioanal. Chem.*, 2003, **375**, (4), 544
70. J. G. Manjunatha, M. Deraman, N. H. Basri, N. S. M. Nor, I. A. Talib and N. Ataollahi, *Comptes Rendus Chim.*, 2014, **17**, (5), 465
71. E. Colín-Orozco, M. T. Ramírez-Silva, S. Corona-Avendaño, M. Romero-Romo and M. Palomar-Pardavé, *Electrochim. Acta*, 2012, **85**, 307
72. J. Aldana-González, M. Palomar-Pardavé, S. Corona-Avendaño, M. G. Montes de Oca, M. T. Ramírez-Silva and M. Romero-Romo, *J. Electroanal. Chem.*, 2013, **706**, 69
73. J. Aldana-González, J. Olvera-García, M. G. Montes de Oca, M. Romero-Romo, M. T. Ramírez-Silva and M. Palomar-Pardavé, *Electrochem. Commun.*, 2015, **56**, 70
74. G. Jiang, T. Jiang, H. Zhou, J. Yao and X. Kong, *RSC Adv.*, 2015, **5**, (12), 9064
75. O. Niwa, G. Xu and Y. Iwasaki, *Electrochem.*, 2006, **74**, (2), 135
76. F. Ye, C. Feng, J. Jiang and S. Han, *Electrochim. Acta*, 2015, **182**, 935
77. G. Camardese, D. Di Giuda, M. Di Nicola, F. Cocciolillo, A. Giordano, L. Janiri and R. Guglielmo, *J. Psychiatr. Res.*, 2014, **51**, 7
78. Y. Zhang, W. Lei, Y. Xu, X. Xia and Q. Hao, *Nanomater.*, 2016, **6**, (10), 178
79. J. Yang, J. R. Strickler and S. Gunasekaran, *Nanoscale*, 2012, **4**, (15), 4594
80. Y. Zhang, Y. Ji, Z. Wang, S. Liu and T. Zhang, *RSC Adv.*, 2015, **5**, (129), 106307
81. L. Hua, X. Wu and R. Wang, *Analyst*, 2012, **137**, (24), 5716
82. C. Shan, H. Yang, D. Han, Q. Zhang, A. Ivaska and L. Niu, *Langmuir*, 2009, **25**, (20), 12030
83. J. Yan, S. Liu, Z. Zhang, G. He, P. Zhou, H. Liang, L. Tian, X. Zhou and H. Jiang, *Coll. Surf. B: Biointer.*, 2013, **111**, 392
84. M. Liu, Q. Chen, C. Lai, Y. Zhang, J. Deng, H. Li and S. Yao, *Biosens. Bioelectron.*, 2013, **48**, 75
85. Q. He, J. Liu, X. Liu, G. Li, P. Deng and J. Liang, *Sensors*, 2018, **18**, (1), 199
86. Y. Shen, Q. Sheng and J. Zheng, *Anal. Methods*, 2017, **9**, (31), 4566
87. Z. Wang, J. Tang, F. Zhang, J. Xia, N. Sun, G. Shi, Y. Xia, L. Xia and L. Qin, *Int. J. Electrochem. Sci*., 2013, **8**, (7), 9967
88. Y. Li, Y. Gu, B. Zheng, L. Luo, C. Li, X. Yan, T. Zhang, N. Lu and Z. Zhang, *Talanta*, 2017, **162**, 80
89. Y. Liu, P. She, J. Gong, W. Wu, S. Xu, J. Li, K. Zhao and A. Deng, *Sensors Actuators B: Chem*., 2015, **221**, 1542
90. L. Zhao, H. Li, S. Gao, M. Li, S. Xu, C. Li, W. Guo, C. Qu and B. Yang, *Electrochim. Acta*, 2015, **168**, 191
91. C. Chen, C. Zhang, X. Gao, Z. Zhuang, C. Du and W. Chen, *Anal. Chem*., 2018, **90**, (3), 1983
92. C. Zhang, L. Li, J. Ju and W. Chen, *Electrochim. Acta*, 2016, **210**, 181
93. M. D. Stoller, S. Park, Y. Zhu, J. An and R. S. Ruoff, *Nano Lett.*, 2008, **8**, (10), 3498
94. L. Lai, J. R. Potts, D. Zhan, L. Wang, C. K. Poh, C. Tang, H. Gong, Z. Shen, J. Lin and R. S. Ruoff, *Energy Environ. Sci.*, 2012, **5**, (7), 7936
95. B. J. Matsoso, B. K. Mutuma, C. Billing, K. Ranganathan, T. Lerotholi, G. Jones and N. J. Coville, *Electrochim. Acta*, 2018, **286**, 29
96. B. J. Matsoso, B. K. Mutuma, C. Billing, K. Ranganathan, T. Lerotholi, G. Jones and N. J. Coville, *J. Electroanal. Chem*., 2019, **833**, 160
97. A. Nsabimana, J. Lai, S. Li, P. Hui, Z. Liu and G. Xu, *Analyst*, 2017, **142**, (3), 478
98. D.-J. Park, J.-H. Choi, W.-J. Lee, S. H. Um and B.-K. Oh, *J. Nanosci. Nanotechnol.*, 2017, **17**, (11), 8012
99. Y. Li, M. Yao, T.-T. Li, Y.-Y. Song, Y.-J. Zhang and S.-Q. Liu, *Anal. Methods*, 2013, **5**, (15), 3635
100. A. Joshi, W. Schuhmann and T. C. Nagaiah, *Sensors Actuators B: Chem.*, 2016, **230**, 544

 © 2019 Johnson Matthey

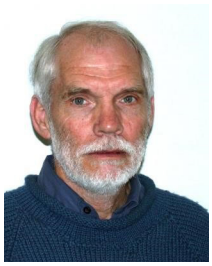
The Authors



Boitumelo J. Matsoso is a postdoctoral fellow (graphene flagship) at Laboratoire des Multimatériaux et Interfaces (UMR 5615 CNRS/UCBL, Université Claude Bernard Lyon 1, France). She is working on the synthesis and characterisation of large area hexagonal boron nitride (*h*-BN) nanomaterials using polymer derived ceramics (PDCs) and chemical vapour deposition (CVD) techniques. She received her BSc in Chemical Technology from the National University of Lesotho, South Africa, in 2013. Her PhD in Chemistry from the University of the Witwatersrand, South Africa, in 2017 was funded by Johnson Matthey, Pretoria, South Africa, for the synthesis of pristine and B/N co-doped graphene films for application as Pt/Pd catalyst supports and in electrochemical sensing.



Tsenolo Lerotholi, a former lecturer at the Molecular Sciences Institute School of Chemistry in University of the Witwatersrand, South Africa, received her PhD from the University of Cambridge, UK, in 2009. Her research interests lie in the field of surface science, focusing primarily on studying fundamental aspects of gas-solid interfaces, such as systems that are important in heterogeneous catalysis, *via* the application of ultra-high-vacuum (UHV) single crystal experiments. She also works on quantitative structure determination of geometric and electronic structures of systems for heterogeneous catalysis, thin films and self-assembled monolayers using low energy electron diffraction (LEED), synchrotron-based photoelectron diffraction and photoelectron spectroscopy (PES).



Neil J. Coville is an Emeritus Professor at the DST-NRF Centre of Excellence in Strong Materials and Molecular Sciences Institute School of Chemistry at the University of the Witwatersrand, South Africa. His research interests can be grouped into a number of (interconnected) areas, including: (i) materials chemistry with emphasis on shaped carbon structures; (ii) heterogeneous catalysis with emphasis on the Fischer-Tropsch reaction; and (iii) the use of carbons in solar cells, in electrochemical sensors as well as catalyst supports in Fischer-Tropsch reactions and fuel cells.



Glenn Jones is currently Core Science Physical and Chemical Modelling Manager at Johnson Matthey, Sonning Common, UK. He holds a PhD from the University of Cambridge, UK and has extensive experience in the field of surface science, catalysis and computational materials chemistry. He moved to the Technical University of Denmark in 2006 to work in the group of Professor Jen K. Nørskov where he got his first taste of industrial collaboration and application of theoretical methods to materials design. After joining Johnson Matthey in 2008, he was awarded a Royal Society Industrial Fellowship in 2010 between Johnson Matthey and University College London, UK. In 2013 he moved to Pretoria, South Africa, to initiate Johnson Matthey's new modelling laboratory in South Africa.

© 2019 Johnson Matthey